PHYSICAL REVIEW B **90**, 115313 (2014)

Strongly nonlinear thermovoltage and heat dissipation in interacting quantum dots

Miguel A. Sierra and David Sánchez
Instituto de Física Interdisciplinar y Sistemas Complejos IFISC (UIB-CSIC), E-07122 Palma de Mallorca, Spain
(Received 31 July 2014; revised manuscript received 12 September 2014; published 26 September 2014)

We investigate the nonlinear regime of charge and energy transport through Coulomb-blockaded quantum dots. We discuss crossed effects that arise when electrons move in response to thermal gradients (Seebeck effect) or energy flows in reaction to voltage differences (Peltier effect). We find that the differential thermoelectric conductance shows a characteristic Coulomb butterfly structure due to charging effects. Importantly, we show that experimentally observed thermovoltage zeros are caused by the activation of Coulomb resonances at large thermal shifts. Furthermore, the power dissipation asymmetry between the two attached electrodes can be manipulated with the applied voltage, which has implications for the efficient design of nanoscale coolers.

DOI: 10.1103/PhysRevB.90.115313 PACS number(s): 73.23.−b, 73.50.Lw, 73.63.Kv, 73.50.Fq

Introduction. In 1993 Staring *et al.* [1] reported an intriguing behavior of the thermovoltage V_{th} generated across a thermally driven Coulomb-blockaded quantum dot. Their observations first indicated an increase of V_{th} with the temperature bias, in agreement with the Seebeck effect. Strikingly enough, for larger heating V_{th} decreased, then vanished for a nonzero thermal difference and finally changed its sign. Very recently, Svensson *et al.* [2] investigated the nonlinear thermovoltage properties of nanowires and made a similar observation. The effect was attributed to a temperature-induced level renormalization because the piled-up charge depends on the applied thermal gradient [3]. However, the potential response was treated as a fitting parameter and single-electron tunneling processes were not properly taken into account.

The subject is interesting for several reasons. First, Coulomb-blockade effects are ubiquitous and govern the transport properties of a large variety of systems: quantum dots [4], molecular bridges [5], carbon nanotubes [6], optical lattices [7], etc. On the other hand, nanostructures are ideal candidates to test novel thermoelectric effects boosting heat-to-work conversion performances [8,9]. Importantly, nonlinearities and rectification mechanisms that lead to the phenomena reported in Refs. [1,2] can be more easily tested in small conductors with strongly energy-dependent densities of states [3,10–22]. We emphasize that there is a close relation between the thermopower of a junction and its heat dissipation properties, as demonstrated in Refs. [23–25] for the linear regime of transport. Therefore, ascertaining the conditions under which thermovoltages acquire a significant nonlinear contribution has broader implications for power generation and cooling applications [26].

We begin our discussion by noticing that vanishing thermovoltages imply the existence of zero thermocurrent states. Unlike voltage-driven currents, which have a definite sign for a bias voltage $V > 0$ and never cross the V axis for normal conductors (an exception is the Hall resistance of an illuminated two-dimensional electron gas [27]), electric transport subjected a thermal gradient θ displays regions of positive or negative thermocurrents depending on the thermopower sign (positive for electronlike carriers, negative for holelike ones [28]). Nevertheless, this is not sufficient for the thermocurrent to cross the θ axis since the thermopower is constant in linear response. Therefore, a strongly negative differential thermoconductance $L = dI/d\theta$ is needed to drive the current I from positive to negative values. This results in an interesting effect—further contact heating may switch off the thermocurrent flowing across the dot. Notably, this is a purely nonlinear thermoelectric effect and has no counterpart with either the voltage-driven case or the linear thermoelectric regime.

Theoretical model. Our results are based on the Anderson model with constant charging energy U,

$$\mathcal{H} = \mathcal{H}_{\rm leads} + \mathcal{H}_{\rm dot} + \mathcal{H}_{\rm tun}\,, \tag{1}$$

where $\mathcal{H}_{\rm leads} = \sum_{\alpha k\sigma} \varepsilon_{\alpha k} C^\dagger_{\alpha k\sigma} C_{\alpha k\sigma}$ is the Hamiltonian of left ($\alpha = L$) and right ($\alpha = R$) reservoirs coupled to the dot. These are described as an electronic band of states with continuous wave number k and spin index $\sigma = \{\uparrow,\downarrow\}$. $\mathcal{H}_{\rm dot} = \sum_\sigma \varepsilon_d d^\dagger_\sigma d_\sigma + U d^\dagger_\uparrow d_\uparrow d^\dagger_\downarrow d_\downarrow$ is the dot Hamiltonian with quasilocalized level ε_d (we consider a single level for definiteness). $\mathcal{H}_{\rm tun} = \sum_{\alpha k\sigma}(V_{\alpha k} C^\dagger_{\alpha k\sigma} d_\sigma + {\rm H.c.})$ is the coupling term that hybridizes dot and leads' states with tunneling amplitudes $V_{\alpha k}$.

The electronic current is given by the time evolution of the expected occupation in one of the reservoirs, $I_\alpha = -ed\langle n_\alpha\rangle/dt$, with $n_\alpha = \sum_{k\sigma} C^\dagger_{\alpha k\sigma} C_{\alpha k\sigma}$. Since the total density commutes with the Hamiltonian of Eq. (1), current conservation demands that $I_L + I_R = 0$ in the steady state. Hence, we can define the current flowing through the system as $I \equiv I_L = -I_R$. Within the Keldysh formalism [29], I is expressed as $I = (e/\pi\hbar){\rm Re}\sum_{k\sigma}\int_{-\infty}^{\infty} dE\, V_{\alpha k} G^<_{\sigma,\alpha k\sigma}(E)$, where $G^<_{\sigma,\alpha k\sigma}(E) = (1/\hbar)\int dE\, G^<_{\sigma,\alpha k\sigma}(t,t') e^{iE(t-t')/\hbar}$ is the Fourier transform of the lesser Green's function $G^<_{\sigma,\alpha k\sigma}(t,t') = \frac{i}{\hbar}\langle C^\dagger_{\alpha k\sigma}(t') d_\sigma(t)\rangle$. Following Ref. [30], the current readily becomes

$$I = -\frac{e}{\pi\hbar}\int dE \sum_\sigma \frac{\Gamma_L\Gamma_R}{\Gamma}{\rm Im}\, G^r_{\sigma,\sigma}(E)[f_L(E) - f_R(E)]\,. \tag{2}$$

G^r is the dot retarded Green's function in the presence of both coupling to the continuum states and electron-electron interactions. $\Gamma_\alpha(E) = 2\pi\rho_\alpha(E)|V_\alpha(E)|^2$ denotes the level broadening due to coupling to the leads (total linewidth $\Gamma = \Gamma_L + \Gamma_R$), with $\rho_\alpha = \sum_k \delta(E - \varepsilon_{\alpha k})$ the α lead density of states. We consider the wide band limit and take Γ_α as constant. Moreover, we assume that both the density of states and the tunneling

probabilities are spin independent (nonmagnetic contacts). Finally, in Eq. (2) $f_\alpha(E) = 1/[1+\exp(E-\mu_\alpha)/(k_BT_\alpha)]$ is the Fermi-Dirac function for lead α with electrochemical potential $\mu_\alpha = E_F + eV_\alpha$ and temperature shift $T_\alpha = T + \theta_\alpha$ (E_F is the common Fermi energy and T is the background temperature).

The spectral function given by $(-1/\pi)\mathrm{Im}\, G^r$ in Eq. (2) can be determined from the equation-of-motion technique followed by a decoupling procedure [31]. We restrict ourselves to the Coulomb-blockade regime ($k_BT, \Gamma \ll U$) and neglect cotunneling and Kondo correlations. This approach yields an excellent characterization of the transport properties of strongly interacting quantum dots for temperatures larger than the Kondo temperature, $T > T_K$. The retarded Green function can be assessed by neglecting the correlators $\langle\langle d^\dagger_{\bar\sigma} C_{\alpha k\bar\sigma} d_\sigma, d^\dagger_\sigma\rangle\rangle \simeq 0$ and $\langle\langle C^\dagger_{\alpha k\bar\sigma} d_{\bar\sigma} d_\sigma, d^\dagger_\sigma\rangle\rangle \simeq 0$ (virtual charge excitations in the dot) and $\langle\langle C_{\alpha k\sigma} C^\dagger_{\beta q\bar\sigma} d_{\bar\sigma}, d^\dagger_\sigma\rangle\rangle \simeq 0$ and $\langle\langle C_{\alpha k\sigma} d^\dagger_{\bar\sigma} C_{\beta q\bar\sigma}, d^\dagger_\sigma\rangle\rangle \simeq 0$ (spin excitations in the leads). These approximations are valid in the Coulomb-blockade regime, for which the charging energy is the largest energy scale in the problem ($\Gamma_\alpha, k_BT < U$). Thus, $G^r_{\sigma,\sigma}(E) = (1-\langle n_{\bar\sigma}\rangle)/(E-\varepsilon_d+i\Gamma/2) + \langle n_{\bar\sigma}\rangle/(E-\varepsilon_d-U+i\Gamma/2)$ depends on the dot occupation for reversed spin $\bar\sigma$, $\langle n_\sigma\rangle = \frac{1}{2\pi i}\int dE\, G^<_{\sigma,\sigma}(E)$. Hence, G^r must be calculated in a self-consistent fashion. Using the Keldysh equation $G^< = i[\Gamma_L f_L(E) + \Gamma_R f_R(E)]|G^r|^2$, we close the system of equations. G^r has two poles at $E = \varepsilon_d$ and $E = \varepsilon_d + U$ broadened by Γ and weighted by $(1-\langle n_{\bar\sigma}\rangle)$ and $\langle n_{\bar\sigma}\rangle$, respectively. This two-peak solution neglects cotunneling effects and Kondo correlations but suffices to treat the Coulomb-blockade regime for not very low temperatures. Importantly, the generalized transmission $(\Gamma_L\Gamma_R/\Gamma)\mathrm{Im}\, G^r_{\sigma,\sigma}(E,\{V_\alpha\},\{\theta_\alpha\})$ depends, quite generally, on both voltage and temperature shifts, as the occupation does, which is a fundamental difference with noninteracting models [32].

We find the spin-dependent occupations

$$\langle n_\sigma\rangle = A(1-\langle n_{\bar\sigma}\rangle) + B\langle n_{\bar\sigma}\rangle\,, \tag{3}$$

$$\langle n_{\bar\sigma}\rangle = A(1-\langle n_\sigma\rangle) + B\langle n_\sigma\rangle\,, \tag{4}$$

where A and B are specified below. The Hamiltonian in Eq. (1) is invariant under spin rotations since no Zeeman splitting is present in the system. Hence, the mean occupation in the dot $\langle n\rangle = \langle n_\sigma\rangle + \langle n_{\bar\sigma}\rangle$ is simply given by

$$\langle n\rangle = \frac{2A}{1+A-B}\,, \tag{5}$$

with $A = (1/2\pi)\int dE\,[\Gamma_L f_L(E) + \Gamma_R f_R(E)]/[(E-\varepsilon_d)^2 + \frac{\Gamma^2}{4}]$ and $B = (1/2\pi)\int dE\,[\Gamma_L f_L(E) + \Gamma_R f_R(E)]/[(E-\varepsilon_d-U)^2 + \frac{\Gamma^2}{4}]$. At equilibrium, $\langle n_\sigma\rangle = \langle n\rangle/2$ ranges between 0 and 1 depending on the value of ε_d, which can be tuned with an external gate potential. As is well known, the dot occupation significantly changes when ε_d crosses the spectral function peaks located at $E = E_F$ and $E = E_F + U$ (degeneracy points). In between, the charge is approximately quantized. We now investigate departures of this behavior when the dot is driven out of equilibrium due to either voltage or thermal gradients.

Voltage-driven case. We consider a voltage bias V symmetrically applied to the leads and set $E_F = 0$ as the reference energy point, $\mu_L = -\mu_R = eV/2$. Inserting Eq. (5) and the G^r expression in Eq. (2), we calculate the I-V characteristic curves for different values of the dot level, see Fig. 1(a). When the single-particle peaks are at resonance with the Fermi energy ($\varepsilon_d = 0$ or $\varepsilon_d = U$), the system behaves as an ohmic junction for voltages around $V = 0$. With increasing V the current reaches a plateau and then increases again when the leads' electrochemical potential realigns with the dot level, which causes an enhancement of the occupation as shown in the inset of Fig. 1(a). This result [33] agrees with phenomenological models of Coulomb blockade [34]. Clearly, the differential conductance $G = dI/dV$ traces show a Coulomb diamond structure as in Fig. 1(b).

The occupation is voltage independent in the particle-hole symmetry point ($\varepsilon_d = -U/2$), in which case the conductance is minimal around $V = 0$. Only for that case the transformation $d \to d^\dagger$ leaves Eq. (1) invariant and the electron density in the dot follows a Fermi distribution. Away from $\varepsilon_d = -U/2$ the dot distribution is not Fermi-like since A and B become doubly stepped functions. Therefore, the occupation [e.g., for $\varepsilon_d = -3U/4$ in the inset Fig. 1(a)] exhibits a nonmonotonic dependence with V and the conductance shows four peaks as seen in Fig. 1(b).

Temperature-driven case. We present in the bottom panel of Fig. 1 the effect of a temperature shift $\Delta T > 0$ applied to one of the electrodes: $\theta_L = \Delta T$ and $\theta_R = 0$ for positive temperature differences $\theta = T_L - T_R > 0$, and $\theta_L = 0$ and $\theta_R = \Delta T$ yielding $\theta < 0$. Noticeably, the thermocurrent curves $I(\theta)$ in Fig. 1(c) lack the Coulomb staircases seen in Fig. 1(a). For $\varepsilon_d = -U/2$ the thermocurrent is identically zero since the dot spectral function of Eq. (2) is symmetric around E_F. At resonance, I grows as the lead gets hotter because more thermally excited electrons are able to tunnel through the nanostructure. A similar response is obtained for level positions between 0 and U at small θ. Further increasing of θ, however, gives rise to dramatic changes. For $\varepsilon_d = -3U/4$ the thermocurrent reaches a maximum and then decreases, crossing the θ axis. In other words, a strong heating of one of the contacts reverses the electronic flow, driving the electrons from the cold to the hot side. This striking behavior is opposite for gate potentials closer to the Fermi energy, see Fig. 1(c) for $\varepsilon_d = -0.15U$. This is a purely nonlinear property of thermoelectric transport that is reflected in the nonmonotonic occupation, see the inset of Fig. 1(c). Remarkably, the value θ where the sign reversal occurs is tunable by varying ε_d. This phenomenon only appears for energies between the peaks of the transmission function ($\varepsilon_d = 0$ and $\varepsilon_d = -U$).

The differential thermoelectric conductance $L = dI/d\theta$ is shown in Fig. 1(d). The Coulomb diamonds of Fig. 1(b) are transformed into a butterfly structure with strong changes of sign across the points $\varepsilon_d = 0$ and $\varepsilon_d = U$ for fixed θ, in agreement with the experiment [2]. The effect is more intense for moderate values of the temperature shift $\theta \lesssim 10T$, a scale dominated by the charging energy. As expected, we obtain $L = 0$ for $\varepsilon_d = -U/2$ independently of θ. Above (below) this symmetry point, L is positive (negative) in the small θ regime, which is a manifestation of the Seebeck effect for electronlike (holelike) carrier transport.

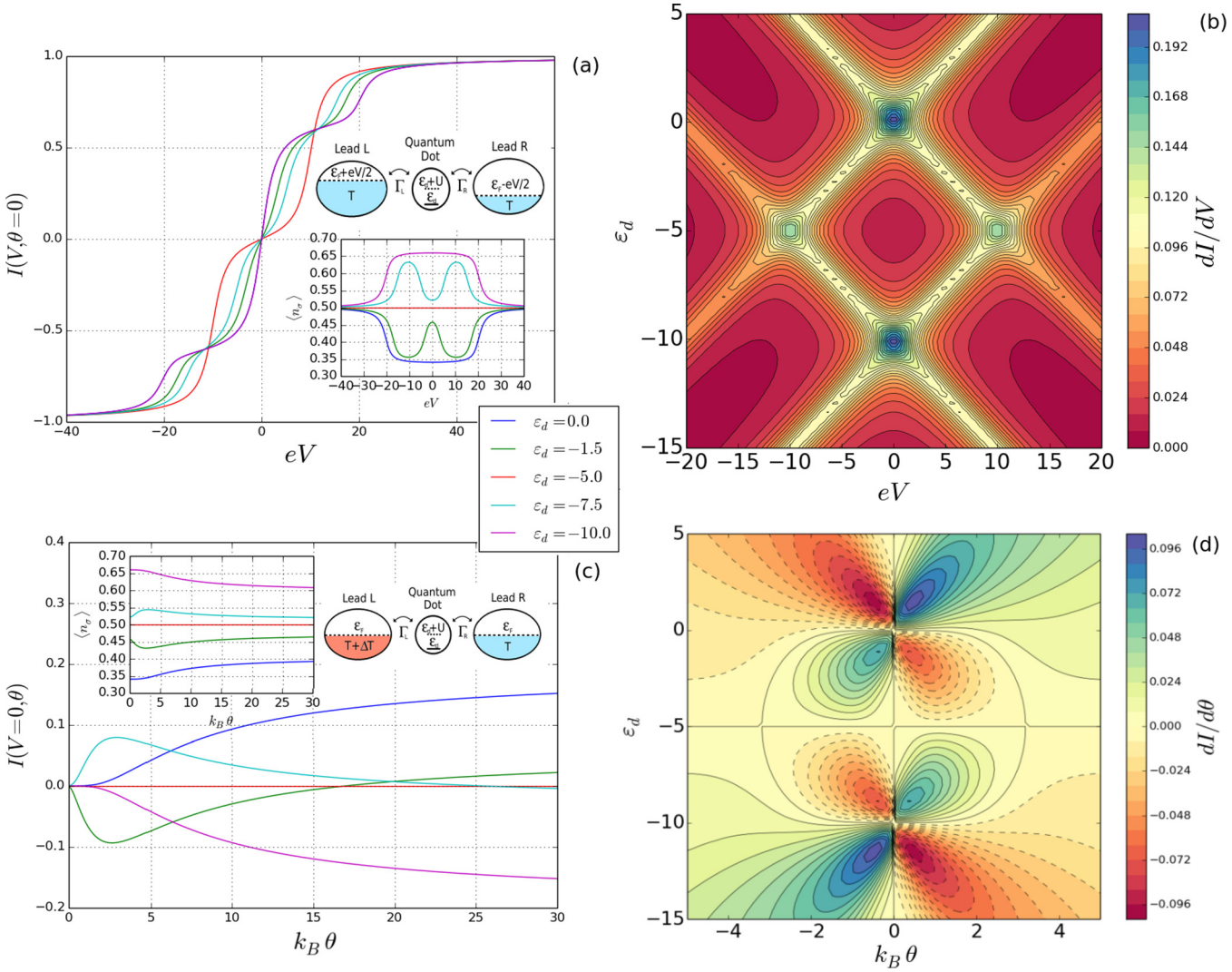

FIG. 1. (Color online) (a) Current-voltage characteristics of a dc-biased single-level Coulomb-blockaded quantum dot (see the sketch) for the indicated gate voltages (level positions). Inset: dot occupation as a function of the voltage bias. (b) Differential conductance versus level position and bias voltage. (c) Thermocurrent of a single-level Coulomb-blockaded quantum dot as a function of the temperature difference shown in the sketch. (d) Differential thermoelectric conductance versus level position and bias voltage. Solid (dashed) lines indicate positive (negative) values. Parameters: charging energy $U = 10$ and background temperature $k_BT = 0.1$. All energies are expressed in terms of $\Gamma_L = \Gamma_R = \Gamma/2$.

Thermocurrent and thermovoltage. The strong nonlinearities in the I-θ curves can be easily understood with a level diagram as sketched in the left panel of Fig. 2. For $\varepsilon_d = -3U/4$ the $E = \varepsilon_d$ ($E = \varepsilon_d + U$) pole lies below (above) E_F (dot-dashed line). If the left lead is heated, thermally excited electrons contribute significantly to the current through the $E = \varepsilon_d + U$ channel and the thermocurrent becomes maximal (point labeled as A in the right side of Fig. 2). As the left contact becomes hotter, the distribution function looses its step form unlike the cold contact. As a consequence, holes (electrons traveling from the right reservoir below E_F) counterbalance the flux from the left side, giving rise to a vanishing thermocurrent at point B. Further increase of θ causes a dominant contribution of holes and I takes on negative values (point C).

The thermovoltage or Seebeck voltage $V_{\rm th}$ is determined from the open-circuit condition $I(V_{\rm th},\theta) = 0$, which we solve numerically to obtain $V_{\rm th} = V_{\rm th}(\theta)$. Except for $\varepsilon_d = -U/2$, the thermovoltage is generally nonzero, see Fig. 3(a). For a small thermal bias, $V_{\rm th}$ is a linear function of θ, yielding a constant thermopower, where the (differential) thermopower is defined as $S(\theta) = dV_{\rm th}/d\theta$, see Fig. 3(b). For ε_d close to $E_F + U$ (E_F), S is positive (negative) for $\theta \to 0$, which can distinguish transport due to electrons or holes. With increasing θ, the thermovoltage grows because larger biases are needed to compensate the thermoelectric flow. Hence, there exists a nice correlation between the $V_{\rm th}(\theta)$ and $I_{\rm th}(\theta)$ curves [cf. Figs. 1(c) and 3(a)]. For any value $\varepsilon_d \in (E_F, E_F + U)$ (except the special point $\varepsilon_d = -U/2$) we always find a θ value such that $V_{\rm th} = 0$. The reason is clear from the above discussion. For the point B marked in Fig. 2 it is unnecessary to apply a voltage bias to counteract the thermal gradient because the thermocurrent is already zero. This effect would also be observable in dot systems with two levels but we remark that the experiments of our interest [1,2] are done in the Coulomb-blockade regime.

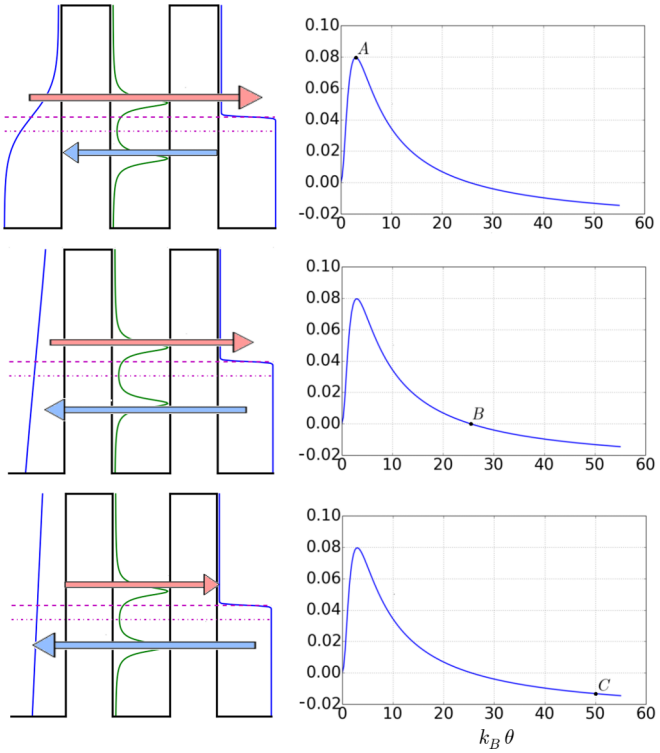

FIG. 2. (Color online) Left: energy diagram corresponding to the current states of the right panel. E_F (ε_d) is indicated with dashed (dotted-dashed) lines. Right: thermocurrent as a function of the temperature difference for $\varepsilon_d = -3U/4$ as taken from Fig. 1(c). Note that the electron flow from the left (right) electrode at point A (C) dominates but exactly cancels out for point B.

Asymmetric dissipation and rectification. The reciprocal effect to the Seebeck conversion is the Peltier effect [35–37], which describes a reversible heat that, unlike the Joule heating, can be used to cool a system by electric means. Recent

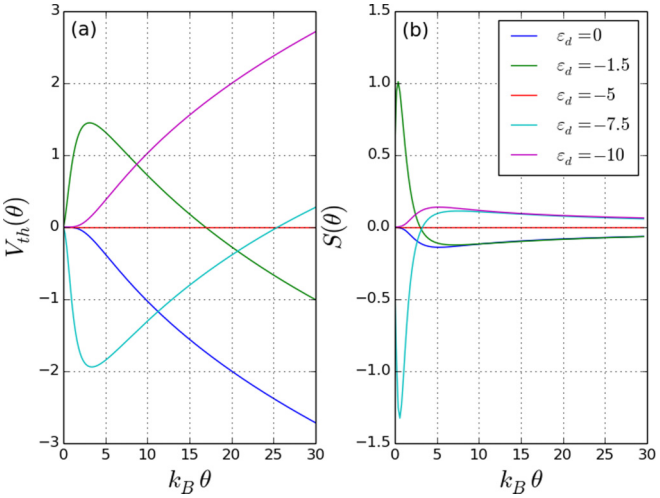

FIG. 3. (Color online) (a) Thermovoltage as a function of the temperature difference for the indicated values of the gate voltages (level positions). (b) Differential thermopower $S = dV_{th}/d\theta$ in units of k_B/e. Parameters: $U = 10$, $k_BT = 0.1$ and energy is given in units of $\Gamma_L = \Gamma_R = \Gamma/2$.

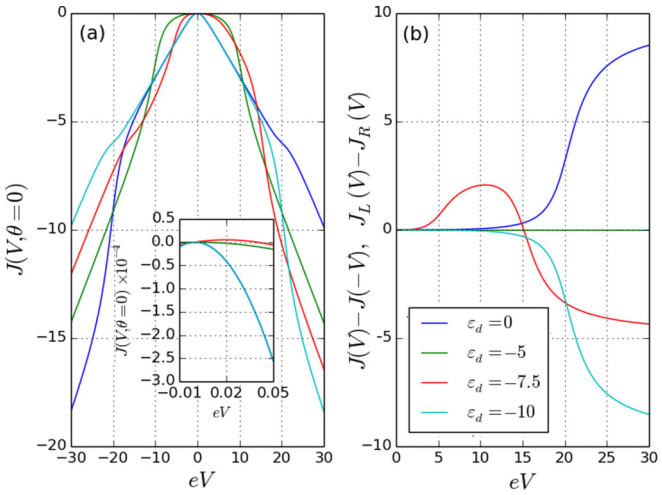

FIG. 4. (Color online) Heat current as a function of applied voltage in the isothermal case $\theta = 0$. Dot level positions are also indicated. Inset: Detail of the dissipated power around zero voltage. (b) Asymmetric dissipation versus voltage bias for the same gate voltages. Parameters: $U = 10$, $k_BT = 0.1$ and energy is given in units of $\Gamma_L = \Gamma_R = \Gamma/2$.

experiments [24] suggest an asymmetric rectification of the generated heat in a voltage-driven atomic-scale junction. These results are interesting because whereas rectification effects are well understood in the electric case [38–44] much less is known about the way power is dissipated in a voltage-biased mesoscopic conductor. The linear part of the rectified heat follows from the linear-response Peltier coefficient. Therefore, the dissipated power can be larger or smaller for a given bias V as compared with its reversed value, depending on whether the atomic resonance lies above or below E_F. However, nonlinear deviations were observed for larger V [24]. Here, we demonstrate that the heat rectification can be tuned with V for a *fixed* position of ε_d.

The heat current is derived from $J_\alpha = d\langle\sum_{k\sigma}\varepsilon_{\alpha k\sigma}C^\dagger_{\alpha k\sigma}C_{\alpha k\sigma}\rangle/dt - \mu_\alpha I_\alpha/e$,

$$J_\alpha = \sum_\sigma \frac{\Gamma_L\Gamma_R}{\pi\hbar\Gamma}\int dE\,(\mu_\alpha - E)\mathrm{Im}\,G^r_{\sigma,\sigma}[f_L(E) - f_R(E)]\,, \tag{6}$$

which satisfies the Joule law $J_L - J_R = IV$. We consider the case where $J \equiv J_L$ is a function of voltage only ($\theta = 0$). Figure 4(a) shows the heat current as a function of V for several values of ε_d. Only for $\varepsilon_d = -U/2$, J exhibits a symmetric behavior, as expected. We observe that the curves quickly depart from the linear regime [see the inset of Fig. 4(b)]. Thus, Joule and higher-order effects start soon to dominate. Interestingly, for $\varepsilon_d = -3U/4$ the heat current shows a nontrivial zero for finite V. The resulting asymmetry under V reversal is apparent for, e.g., $\varepsilon_d = U$. Our results also show that the heat current is invariant under the joint transformation $V \to -V$ and $\varepsilon_d \to -\varepsilon_d - U$ (see, e.g., the $\varepsilon_d = 0$ and $\varepsilon_d = -U$ cases).

In Fig. 4(b) we depict the rectification factor $J(V) - J(-V)$ for different dot level positions. At resonance ($\varepsilon_d = 0$),

the rectification is always positive, i.e., the dissipation is larger for $V > 0$ than for $V < 0$ and increases with voltage. Clearly, for $V > 0$ heat can flow through either $E = 0$ or $E = U$ peaks while for $V < 0$ energy can be transported through the $E = 0$ resonance only. The situation is reversed for $\varepsilon_d = -U$. The dissipation is now larger for negative voltages than for positive polarities. More importantly, the rectification factor can change its sign for a given value of ε_d, as indicated in Fig. 4(b) for $\varepsilon_d = -3U/4$. Notice that this is a purely nonlinear effect. While in the linear case the rectification can be changed with tuning ε_d and this effect heavily depends on the transmission energy dependence [24], here a voltage scan leads to a value where the transformation $V \to -V$ leaves J invariant. Furthermore, it is straightforward to show that the power difference between the left and right electrodes for a given bias, $J_L(V) - J_R(V)$, equals $J(V) - J(-V)$ if the dot spectral function is symmetric under V reversal. Our system indeed shows this property for symmetric couplings, $\Gamma_L = \Gamma_R$ [see the inset of Fig. 1(a), where the occupation is an even function of V]. Therefore, heat can be dissipated equally between the leads ($J_L = J_R$) for $V \neq 0$ [see Fig. 4(b) for $\varepsilon_d = -3U/4$], despite the fact that the transmission strongly depends on energy, unlike the linear case [24]. This is again an effect that can be observed in the nonlinear regime of transport only.

Conclusion. We have examined a counterintuitive phenomenon seen in experiments—with increasingly thermal gradient applied to a quantum dot the created thermovoltage diminishes and even becomes zero for a nonzero temperature bias. We have shown that the effect is due to the combined influence of the two peaks arising from a Coulomb-blockade level. Furthermore, we predict a reciprocal effect—the power rectification becomes zero for a finite voltage, which can be relevant for the design of nanodevices with controllable dissipation. Further work should clarify the role of (higher-order) cotunneling processes [45,46] and Kondo interactions [47–49]. The effects discussed here are robust and should not depend on the theoretical method. In particular, we expect similar conclusions using an orthodox model [34] or a master equation framework [50].

Acknowledgments. We thank R. López for useful discussions. Work supported by MINECO under Grant No. FIS2011-23526.

[1] A. A. M. Staring, L. W. Molenkamp, B. W. Alphenaar, H. van Houten, O. J. A. Buyk, M. A. A. Mabesoone, C. W. J. Beenakker, and C. T. Foxon, Europhys. Lett. **22**, 57 (1993).
[2] S. Fahlvik Svensson, E. A. Hoffmann, N. Nakpathomkun, P. M. Wu, H. Q. Xu, H. A. Nilsson, D. Sánchez, V. Kashcheyevs, and H. Linke, New J. Phys. **15**, 105011 (2013).
[3] D. Sánchez and R. López, Phys. Rev. Lett. **110**, 026804 (2013).
[4] L. P. Kouwenhoven, C. M. Marcus, P. L. McEuen, S. Tarucha, R. M. Westervelt, and N. S. Wingreen, in *NATO ASI Conference Proceedings*, edited by L. P. Kouwenhoven, G. Schön, and L. L. Sohn (Kluwer, Dordrecht, 1997), p. 105.
[5] J. Park *et al.*, Nature (London) **417**, 722 (2002).
[6] H. W. Postma, T. Teepen, Z. Yao, M. Grifoni, and C. Dekker, Science **293**, 76 (2001).
[7] P. Cheinet, S. Trotzky, M. Feld, U. Schnorrberger, M. Moreno-Cardoner, S. Fölling, and I. Bloch, Phys. Rev. Lett. **101**, 090404 (2008).
[8] Y. Dubi and M. Di Ventra, Rev. Mod. Phys. **83**, 131 (2011).
[9] G. Benenti, G. Casati, T. Prosen, and K. Saito, arXiv:1311.4430.
[10] D. Boese and R. Fazio, Europhys. Lett. **56**, 576 (2001).
[11] M. Krawiec and K. I. Wysokiński, Phys. Rev. B **75**, 155330 (2007).
[12] David M.-T. Kuo and Y. C. Chang, Phys. Rev. B **81**, 205321 (2010).
[13] R. S. Whitney, Phys. Rev. B **87**, 115404 (2013).
[14] J. Meair and P. Jacquod, J. Phys.: Condens. Matter **25**, 082201 (2013).
[15] R. López and D. Sánchez, Phys. Rev. B **88**, 045129 (2013).
[16] S. Hershfield, K. A. Muttalib, and B. J. Nartowt, Phys. Rev. B **88**, 085426 (2013).
[17] J. Matthews, F. Battista, D. Sánchez, P. Samuelsson, and H. Linke, arXiv:1306.3694.
[18] S.-Y. Hwang, D. Sánchez, M. Lee, and R. López, New J. Phys. **15**, 105012 (2013).
[19] P. Dutt and K. Le Hur, Phys. Rev. B **88**, 235133 (2013).
[20] R. S. Whitney, Phys. Rev. Lett. **112**, 130601 (2014).
[21] N. A. Zimbovskaya, arXiv:1405.6968.
[22] J. Azema, P. Lombardo, and A.-M. Daré, arXiv:1407.5065.
[23] M. Leijnse, M. R. Wegewijs, and K. Flensberg, Phys. Rev. B **82**, 045412 (2010).
[24] W. Lee, K. Kim, W. Jeong, L. A. Zotti, F. Pauly, J. C. Cuevas, and P. Reddy, Nature (London) **498**, 209 (2013); L. A. Zotti, M. Bürkle, F. Pauly, W. Lee, K. Kim, W. Jeong, Y. Asai, P. Reddy, and J. C. Cuevas, New J. Phys. **16**, 015004 (2014).
[25] O. Entin-Wohlman, J.-H. Jiang, and Y. Imry, Phys. Rev. E **89**, 012123 (2014).
[26] F. Giazotto, T. T. Heikkilä, A. Luukanen, A. M. Savin, and J. P. Pekola, Rev. Mod. Phys. **78**, 217 (2006).
[27] R. G. Mani, J. H. Smet, K. von Klitzing, V. Narayanaimurti, W. B. Johnson, and V. Umansky, Nature (London) **420**, 646 (2002).
[28] P. Reddy, S. Y. Jang, R. A. Segalman, and A. Majumdar, Science **315**, 1568 (2007).
[29] See, e.g., H. Haug and A.-P. Jauho, *Quantum Kinetics in Transport and Optics of Semiconductors* (Springer, Berlin, 2007).
[30] Y. Meir and N. S. Wingreen, Phys. Rev. Lett. **68**, 2512 (1992).
[31] A. C. Hewson, Phys. Rev. **144**, 420 (1966).
[32] P. N. Butcher, J. Phys.: Condens. Matter **2**, 4869 (1990).
[33] Y. Meir, N. S. Wingreen, and P. A. Lee, Phys. Rev. Lett. **66**, 3048 (1991).
[34] C. W. J. Beenakker, Phys. Rev. B **44**, 1646 (1991).
[35] I. O. Kulik, J. Phys.: Condens. Matter **6**, 9737 (1994).
[36] E. N. Bogachek, A. G. Scherbakov, and U. Landman, Phys. Rev. B **60**, 11678 (1999).

[37] M. Zebarjadi, K. Esfarjani, and A. Shakouri, Appl. Phys. Lett. **91**, 122104 (2007).
[38] A. M. Song, A. Lorke, A. Kriele, J. P. Kotthaus, W. Wegscheider, and M. Bichler, Phys. Rev. Lett. **80**, 3831 (1998).
[39] H. Linke, W. D. Sheng, A. Svensson, A. Lofgren, L. Christensson, H. Q. Xu, P. Omling, and P. E. Lindelof, Phys. Rev. B **61**, 15914 (2000).
[40] I. Shorubalko, H. Q. Xu, I. Maximov, P. Omling, L. Samuelson, and W. Seifert, Appl. Phys. Lett. **79**, 1384 (2001).
[41] R. Fleischmann and T. Geisel, Phys. Rev. Lett. **89**, 016804 (2002).
[42] M. Büttiker and D. Sánchez, Phys. Rev. Lett. **90**, 119701 (2003).
[43] T. González, B. G. Vasallo, D. Pardo, and J. Mateos, Semicond. Sci. Technol. **19**, S125 (2004).
[44] B. Hackens, L. Gence, C. Gustin, X. Wallart, S. Bollaert, A. Cappy, and V. Bayot, Appl. Phys. Lett. **85**, 4508 (2004).
[45] M. Turek and K. A. Matveev, Phys. Rev. B **65**, 115332 (2002).
[46] K. Torfason, A. Manolescu, S. I. Erlingsson, and V. Gudmundsson, Physica E **53**, 178 (2013).
[47] B. Dong and X. L. Lei, J. Phys.: Condens. Matter **14**, 11747 (2002).
[48] R. Scheibner, H. Buhmann, D. Reuter, M. N. Kiselev, and L. W. Molenkamp, Phys. Rev. Lett. **95**, 176602 (2005).
[49] T. A. Costi and V. Zlatić, Phys. Rev. B **81**, 235127 (2010).
[50] C. Timm, Phys. Rev. B **77**, 195416 (2008).